Advanced Physics Laboratory

“Electron-Paramagnetic Resonance (EPR)”

University of Leipzig
Department of Physics and Geosciences
2001

BASIC THEORY OF PULSE EPR

 Fourier-transform EPR

 The magnetization vector picture. Bloch equations

 Pulse and FID

 A primer of spin quantum mechanics

 Polarization, coherence, and the density matrix

 Fourier transformation. Dead time artifacts

 The Hahn echo. Separation of signals by phase cycling.

CW EPR works Nicely- Why FT EPR?

Or: Why did FT NMR completely supersede CW NMR?

1. Sensitivity

- a CW spectrometer measures baseline most of the time (if lines are narrow)
- an FT spectrometer measures signal all the time (multiplex advantage)

EPR samples are few and far between, where this is significant

2. Spin choreography and 2D experiments

- isolate interactions and detect correlations that are not observable by CW methods

3. Time resolution (response time)

- about 10 ns, much better than in CW EPR (field modulation)

SCOPE OF FT EPR

Requirements on spectrum

- spectral width < 100 MHz (35 G)
- line width < 3 MHz (1 G)

Typical systems

- organic radicals in solution
- exchange narrowed lines or conduction electrons
- proton-free single crystals
- disordered solids only if

  either high local symmetry (cubic, tetrahedral)

  or virtually no hyperfine couplings (silica glass)

  or pathological cases (fullerenes, Mn^{2+} central lines)

Motion of Spins in Magnetic Fields

Thermal Equilibrium

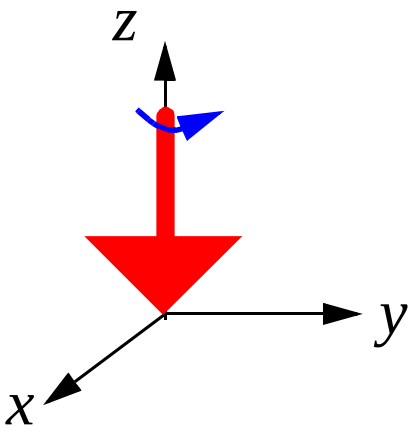

$$\sigma_{eq} = -S_z$$

M.W. Pulse

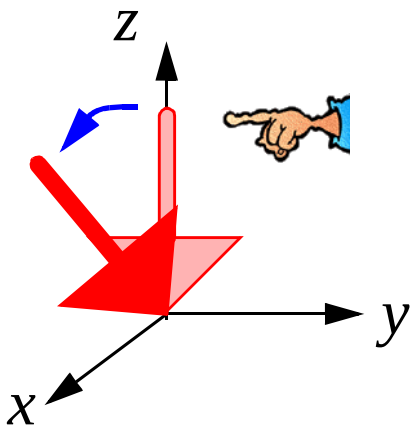

$$-S_z \xrightarrow{\beta S_x} -\cos(\beta)S_z + \sin(\beta)S_y$$

Precession

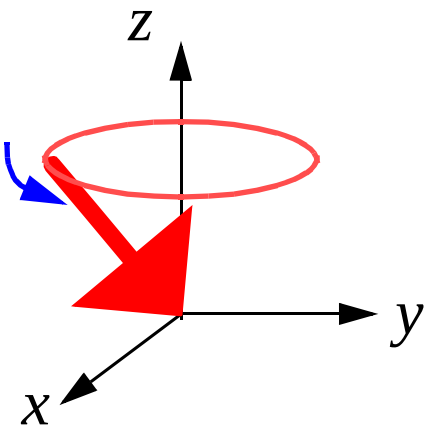

$$S_y \xrightarrow{\omega_S t\, S_x} \cos(\omega_S t)S_y - \sin(\omega_S t)S_x$$

Mathematical Description of Spin Motion
Precession in a Static Field

For static as well as time-dependent magnetic fields **B:**

$$\frac{d\mathbf{M}}{dt} = \frac{g\mu_B}{\hbar}\mathbf{M}\times\mathbf{B}$$

interaction is maximum if spin and field are perpendicular

Vector product $\mathbf{M}\times\mathbf{B}$

$$|\mathbf{M}\times\mathbf{B}| = \sin(\theta)|\mathbf{M}||\mathbf{B}|$$

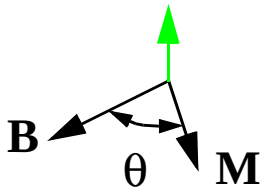

For a static field B_0 along z:

$$\frac{dM_x}{dt} = \frac{g\mu_B B_0}{\hbar}M_y = -\omega_S M_y$$

$$\frac{dM_y}{dt} = -\frac{g\mu_B B_0}{\hbar}M_x = \omega_S M_x$$

$$\frac{dM_z}{dt} = 0$$

MATHEMATICAL DESCRIPTION OF SPIN MOTION DURING M.W. PULSES (I)

Linearly polarized m.w. field $\mathbf{B}_1(t)$:

$$2\mathbf{B}_1(t) = 2\cos(\omega_{mw}t)B_1\mathbf{e}_X$$

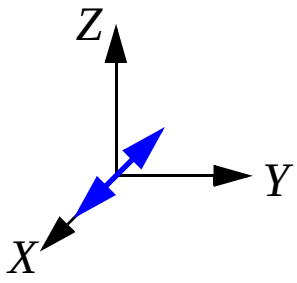

is the sum of two circularly polarized components:

field rotation follows spin precession

field rotation against spin precession

$$\mathbf{B}_{1r}(t) = \cos(\omega_{mw}t)B_1\mathbf{e}_X + \sin(\omega_{mw}t)B_1\mathbf{e}_Y$$

$$\mathbf{B}_{1l}(t) = \cos(\omega_{mw}t)B_1\mathbf{e}_X - \sin(\omega_{mw}t)B_1\mathbf{e}_Y$$

now let the frame rotate with the m.w. frequency about Z:

$$\mathbf{B}_1 = B_1\mathbf{e}_x$$

$$-\frac{g\mu_B B_1}{\hbar} = \omega_1$$

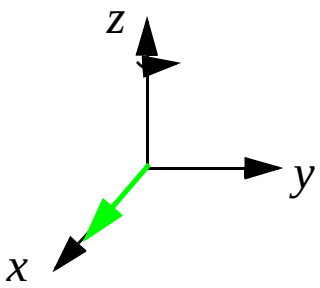

MATHEMATICAL DESCRIPTION OF SPIN MOTION DURING M.W. PULSES (II)

Equations of motion in the rotating frame:

$$\frac{dM_x}{dt} = -\Omega_S M_y$$

$$\frac{dM_y}{dt} = \Omega_S M_x - \omega_1 M_z$$

$$\frac{dM_z}{dt} = \omega_1 M_y$$

$$\Omega_S = \omega_S - \omega_{mw}$$

near resonance:

$$\omega_1 \gg \Omega_S$$

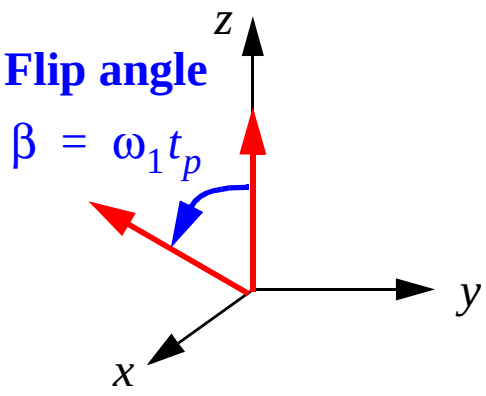

Flip angle

$\beta = \omega_1 t_p$

We detect transverse magnetization (M_x and/or M_y).

Maximum signal is thus obtained for $\beta = \pi/2$ (90°)

$\Rightarrow$ Most pulse sequences start with a $\pi/2$ pulse:

$$\sigma_{eq} = -S_z \xrightarrow{\frac{\pi}{2}S_x} S_y$$

THE BLOCH EQUATIONS- A COMPLETE DESCRIPTION OF FT-EPR FOR $S=1/2$

Longitudinal relaxation:

- spins exchange energy with their environment (spin-lattice relaxation)
- M_z approaches equilibrium value M_0 with time constant T_1

Bloch equations:

$$\frac{dM_x}{dt} = -\Omega_S M_y - \frac{M_x}{T_2}$$

$$\frac{dM_y}{dt} = \Omega_S M_x - \omega_1 M_z - \frac{M_y}{T_2}$$

$$\frac{dM_z}{dt} = \omega_1 M_y - \frac{M_z - M_0}{T_1}$$

$$\frac{1}{T_2} = \frac{1}{T_2'} + \frac{1}{2T_1}$$

For fast motion in liquid phase:

$$T_2 = T_1$$

Trajectory of **M** after π/2 pulse:

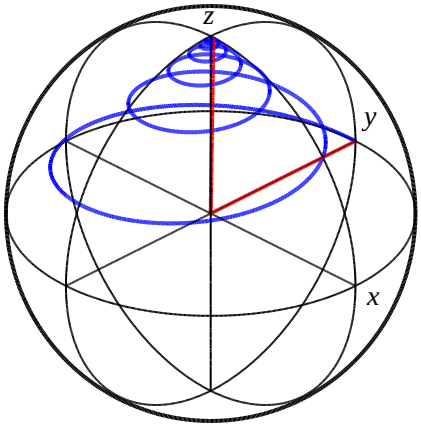

THE FREE INDUCTION DECAY (FID) SIGNAL

Quadrature detection: Looking at both M_x and M_y

Real part:

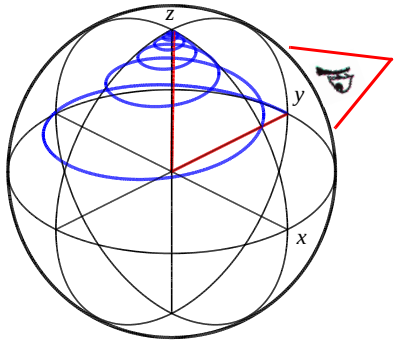

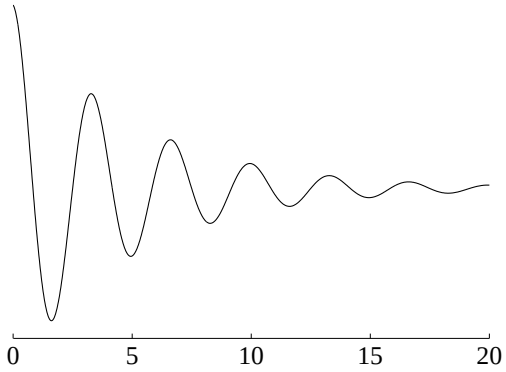

$$\cos(\Omega_S t)\exp\left(-\frac{t}{T_2}\right)$$

Imaginary part:

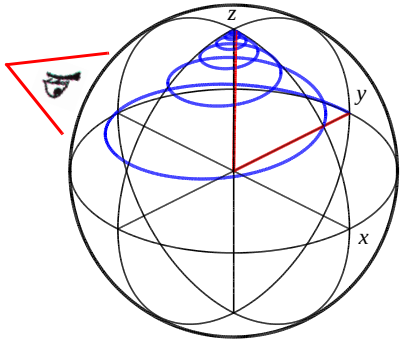

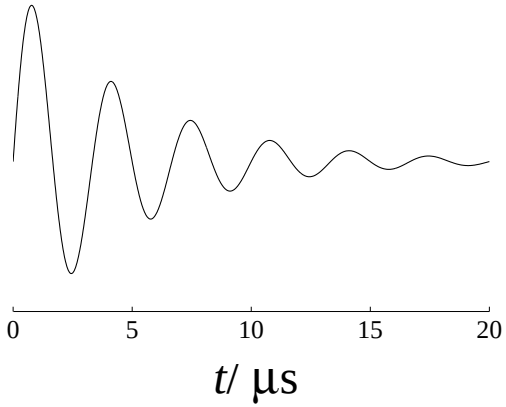

$$\sin(\Omega_S t)\exp\left(-\frac{t}{T_2}\right)$$

SPIN QUANTUM MECHANICS: THE WAVE FUNCTION AND MACROSCOPIC MAGNETIZATION

Spin wave function: $|\psi\rangle = c_\alpha|\alpha\rangle + c_\beta|\beta\rangle$

c_α and c_β are *complex* numbers

Populations:

$|\alpha\rangle$ or $|1/2\rangle$ $p_\alpha = |c_\alpha|^2$

$|\beta\rangle$ or $|-1/2\rangle$ $p_\beta = |c_\beta|^2$

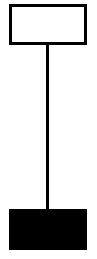

Magnetization of an ensemble of *N* spins *S*=1/2 in a *pure* state:

Operators:

$$M_x = \frac{-g_e\mu_B\hbar N}{2}(c_\alpha^* c_\beta + c_\alpha c_\beta^*)$$

$$M_y = \frac{-ig_e\mu_B\hbar N}{2}(c_\alpha^* c_\beta - c_\alpha c_\beta^*)$$

Coherence S_x, S_y

$$M_z = \frac{-g_e\mu_B\hbar N}{2}(|c_\alpha|^2 - |c_\beta|^2)$$

Polarization S_z

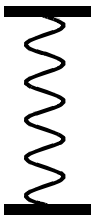

SPIN QUANTUM MECHANICS: MIXED STATES AND THE DENSITY MATRIX

Pure state: All spins in the ensemble have the same wave function $|\psi\rangle$

Mixed state: There are *n* subensembles with different wave functions $|\psi_i\rangle$

Macroscopic properties are now derived from *ensemble averages*, e.g. $\overline{|c_\alpha|^2} = \sum_i p_i \left|c_\alpha^{(i)}\right|^2$

Magnetization of an ensemble of *N* spins *S*=1/2 in a *mixed* state:

$$M_x = \frac{-g_e \mu_B \hbar N}{2} \sum_i p_i (c_\alpha^{(i)*} c_\beta^{(i)} + c_\alpha^{(i)} c_\beta^{(i)*})$$

$$M_y = \frac{-i g_e \mu_B \hbar N}{2} \sum_i p_i (c_\alpha^{(i)*} c_\beta^{(i)} - c_\alpha^{(i)} c_\beta^{(i)*})$$

$$M_z = \frac{-g_e \mu_B \hbar N}{2} \sum_i p_i (\left|c_\alpha^{(i)}\right|^2 - \left|c_\beta^{(i)}\right|^2)$$

Density matrix:

$$\sigma = \begin{pmatrix} \overline{|c_\alpha|^2} & \overline{c_\alpha c_\beta^*} \\ \overline{c_\alpha^* c_\beta} & \overline{|c_\beta|^2} \end{pmatrix}$$

	$\|\alpha\rangle$	$\|\beta\rangle$
$\langle\alpha\|$	σ_{11}	σ_{12}
$\langle\beta\|$	σ_{21}	σ_{22}

Populations

Coherence

$\sigma_{12} = \sigma_{21}^*$

SPIN QUANTUM MECHANICS: THE DENSITY MATRIX FOR LARGER SPIN SYSTEMS

Example: S_A=1/2, S_B=1/2 system

	$\|\alpha\alpha\rangle$	$\|\beta\alpha\rangle$	$\|\alpha\beta\rangle$	$\|\beta\beta\rangle$
$\langle\alpha\alpha\|$	$P_{\alpha\alpha}$	SQC^A	SQC^B	DQC
$\langle\beta\alpha\|$	SQC^A	$P_{\alpha\beta}$	ZQC	SQC^B
$\langle\alpha\beta\|$	SQC^B	ZQC	$P_{\beta\alpha}$	SQC^A
$\langle\beta\beta\|$	DQC	SQC^B	SQC^A	$P_{\beta\beta}$

coherence order *p*

P_{kj} **populations** 0

SQC **single-quantum coherence** -1,1
coherence on allowed transitions

ZQC **zero-quantum coherence** 0

DQC **double-quantum coherence** -2,2
coherences on forbidden transitions

$$\sigma = \sum_{i=1}^{n} p_i |\psi_i\rangle\langle\psi_i| = \sum_{kl} \overline{c_l^* c_k}\, |l\rangle\langle k|$$

Expectation value of the observable *A*:

$$\langle A\rangle = \sum_k \langle k|\sigma A|k\rangle = \mathrm{Tr}\{\sigma A\}$$

FOURIER TRANSFORMATION FOR SIGNAL PROCESSING OF FIDS

Orthogonality relations of trigonometric functions, e.g.

$$\int_{-\infty}^{\infty} \cos(\omega_a t)\cos(\omega_b t)dt = \begin{cases} 1 \text{ for } \omega_a = \omega_b \\ 0 \text{ for } \omega_a \neq \omega_b \end{cases}$$

can be used for frequency analysis:

Cosine- FT

$$S(\omega) = \int_0^{\infty} V(t)\cos(\omega t)dt$$

Complex FT

$$S(\omega) = \int_0^{\infty} V(t)e^{-i\omega t}dt$$

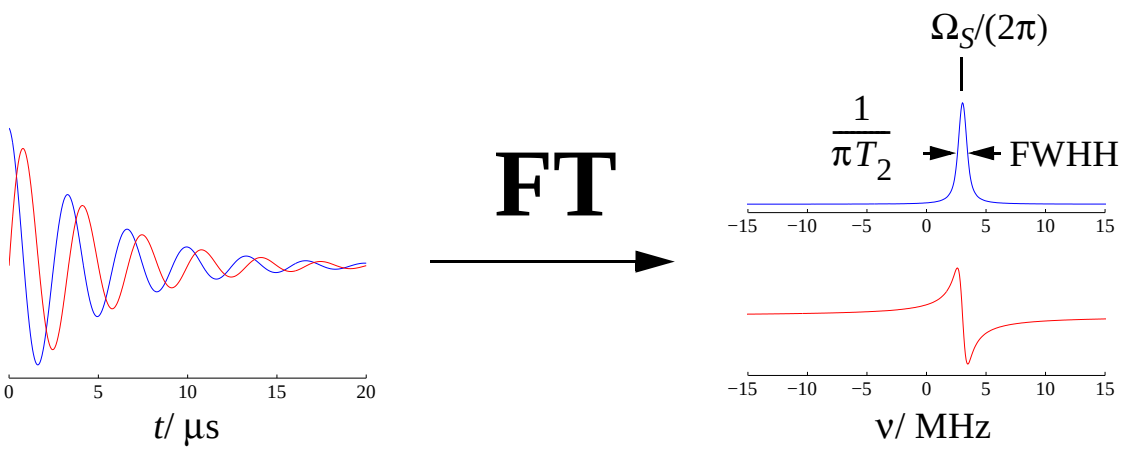

RECEIVER DEADTIME I: PHASE DISTORTIONS

Some receiver deadtime passes after the pulse before detection is possible

- receiver is saturated by pulse ringing
- signal is distorted by pulse ringing

Simulated nitroxide FID (3 lines)

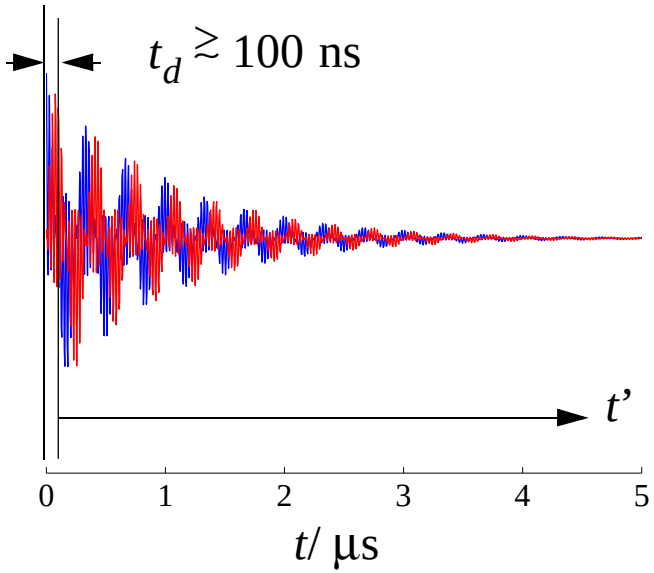

FT(t')

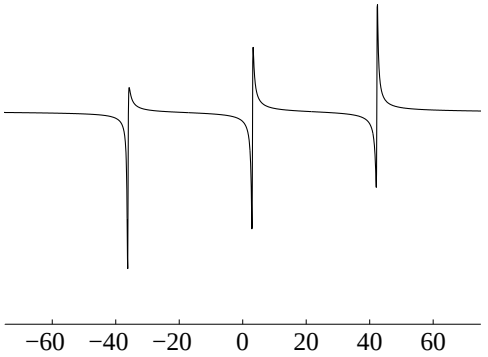

$\times \exp(-i\omega t_d)$

phase correction

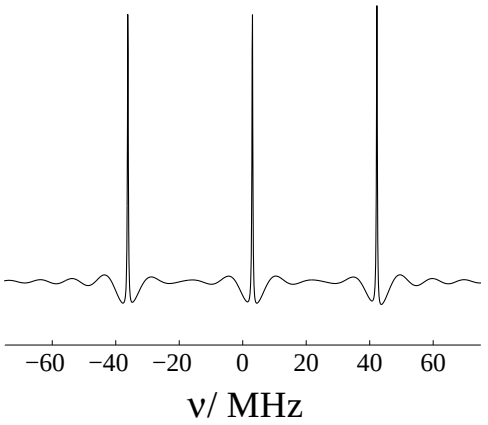

RECEIVER DEADTIME II: LOSS OF BROAD SIGNALS

Consider the spectrum of a nitroxide free radical in viscous solution:

CW EPR (simulation)

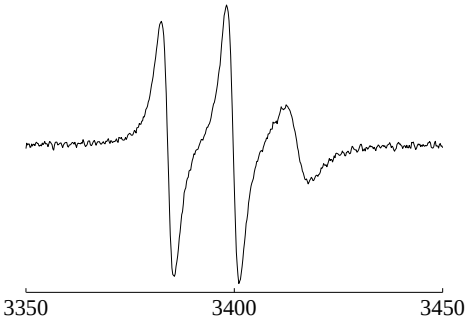

Hypothetical FT EPR spectrum

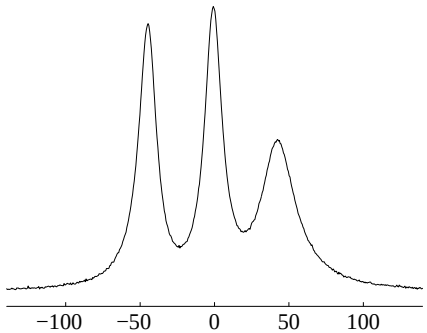

Simulated FID

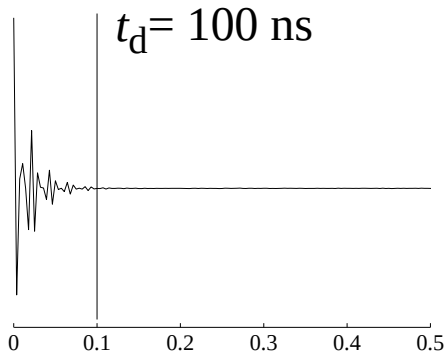

FT EPR spectrum considering deadtime

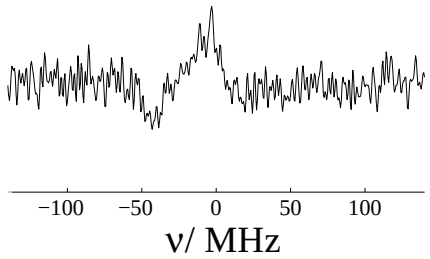

PULSE EPR ON SOLIDS

FT EPR usually does not work

- only a small part of the spectrum can be excited at once
- FIDs usually decay within deadtime

The electron spin echo (ESE) overcomes both problems, and

- gives access to interactions hidden by line broadening
- allows for separation of interactions and 2D spectroscopy by multi-pulse techniques
- is the basis for an alternative to ENDOR for studying hyperfine interactions (ESEEM)

ELECTRON SPIN ECHO: BASIC IDEA AND APPLICATION TO LIQUIDS

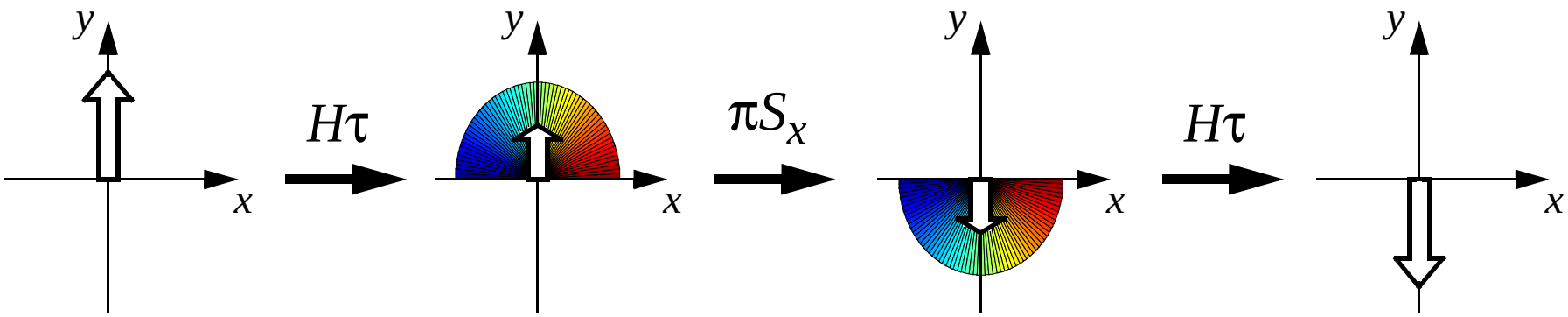

Pulse sequence

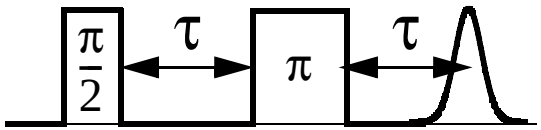

Application to liquids

- for $\tau > t_d$ no phase distortions by deadtime

Problem

- FID is not completely quenched by π pulse
- echo is distorted by superposed FID

SEPARATION OF SIGNAL CONTRIBUTIONS BY PHASE CYCLING

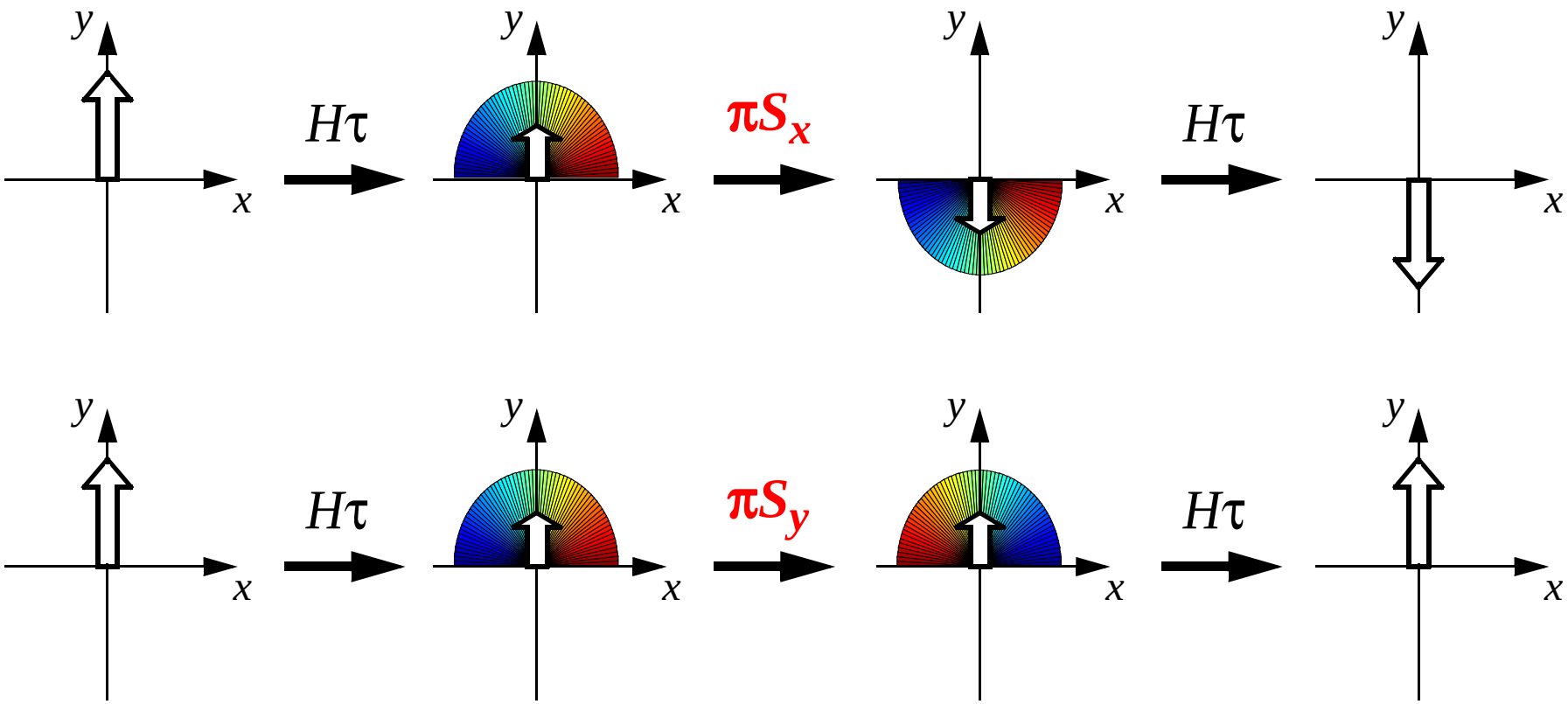

- echo changes sign, but FID is not influenced
- difference of signals is pure echo contribution, sum is pure FID contribution

Tasks

1. Working with the Reflex Klystron

1.1 Measure (for one klystron mode) the dependence $N = N(U_R)$, where U_R is the voltage of the reflector, and the dependence $\nu = \nu(U_R)$, where ν is the klystron frequency (the current through the diode is proportional to the klystron power N).

1.2 Represent the individual vibrational modes of the klystron oscillographically by modulating the reflector voltage with the sweep-wave of the oscilloscope. Adapt the klystron.

1.3 Tune the klystron to the resonance frequency of the measuring cavity and determine the resonance frequency of the cavity:
a) Without sample
b) With the DPPH-sample
c) With the $CuSO_4 \cdot 5H_2O$-sample

2. Verification of the Electron Spin Resonance at the paramagnetic Substance $CuSO_4 \cdot 5H_2O$

2.1 Record the absorption line of $CuSO_4 \cdot 5H_2O$ point by point. Choose an appropriate step width of the magnetic field (bridge matching via the tuning circuit 6 in the side arm S1, at the block diagram in figure 18 the switches 1 and 2 are in the position 1).

2.2 Determine the resonance field strength, the line width, and the g-factor of the substance and estimate the measuring errors.

3. Methodical Exercises

3.1 Record the EPR-signal of DPPH (10mg sample) oscillographically and try to maximize the signal by adjusting the different tuning elements.
Check with the measured microwave frequency and the known g-factor (g=2.0037) the resonance frequency determined by you. Estimate the errors of the measurement of the magnetic field strength.

3.2 Record the EPR-signal of DPPH (0.5mg sample) oscillographically and estimate the responsivity (smallest number of detectable paramagnetic centres per line width at a signal noise ratio of 1:1) after you tuned again to the maximal signal height.

3.3 Measure the g-factor of the ultramarine(UM) sample.

3.4 Investigate the influence of the modulation of the amplitude of the magnetic field H_M on the EPR-signal displayed on the oscilloscope. Use the UM- and the DPPH-sample!

a) Record the EPR-spectrum of the UM- and the DPPH-sample with the help of the storage oscilloscope for the following modulation currents: 200, 400, 500, 600, 700, 800, and 1000mA. Heed the manual of the oscilloscope at the working place, too.
For the analysis it is always useful to tune exactly to the DPPH resonance.

b) Determine a calibration curve for the modulation field strength $H_M[G] = f(I_M[mA])$ using the measured gaps between the lines. What physical meaning has the calibration curve?

4. EPR-Measurements at a $[Cr(H_2O)_6]^{3+}$ - centre in GASH

In this task one should do a complete analysis of the EPR-spectrum of the $[Cr(H_2O)_6]^{3+}$ - centre in GASH. In order to understand the questions connected to the complete analysis, one should read and understand the Section 3. The interpretation of the spectra is based on the assumption, that (because of the doping of the GASH host materials with $Cr_2(SO_4)\cdot 12H_2O$) the $[Al(H_2O)_6]^{3+}$ - groups are replaced by $[Cr(H_2O)_6]^{3+}$ - centres.

4.1 Record the EPR-spectrum of both crystalline samples in an arbitrary orientation. Answer the following questions for yourself:

a) How many EPR-lines are expected for the $[Cr(H_2O)_6]^{3+}$ - centre?
b) Which transitions are expected ("allowed" and "forbidden" transitions)?
c) Number of the observed $[Cr(H_2O)_6]^{3+}$ - centres?

4.2 For the determination of the principle values and the principle axes contained in the interaction tensor of the spin Hamilton operator it is necessary, to investigate the angular dependence of the EPR-spectrum.

4.2.1 Measure the crystal 1 with a step width of 5° in a range of 120°.

4.2.2 Measure the crystal 2 with a step width of 5° in a range of 120°.

4.2.3 Draw the angular plots:

a) $H_R = H_R(\theta)$ crystal 1
b) $H_R = H_R(\phi)$ crystal 2

University of Illinois at Urbana-Champaign Department of Physics

Physics 303 Laboratory

ELECTRON PARAMAGNETIC RESONANCE

Contents

Revised 1/1993.

I. PURPOSE

The purpose of this experiment is to become familiar with the technique of electron paramagnetic resonance and to measure the g-factor and the hyperfine splitting constant for the ion V^{2+} in a MgO crystal.

II. REFERENCES

1. A. C. Melissinos, Experiments in Modern Physics, Academic Press, 1966, P. 374.

2. T. W. Orton, Electron Paramagnetic Resonance, Gordon and Breach, 1968.

3. A. Abragam and B. Bleaney, Electron Paramagnetic Resonance of Transition Ions, Oxford, 1970, a standard reference in the field.

4. R. S. Alger, Electron Paramagnetic Resonance-Techniques and Applications, John Wiley, 1968, good on applications including solids, especially F-centers.

5. C. Kittel, Introduction to Solid State Physics, J. Wiley, 1976, Chap. 14.

III. INTRODUCTION

A. Principles of Electron Spin Resonance

Electron paramagnetic resonance is a branch of spectroscopy in which electromagnetic radiation of microwave frequency is absorbed by atoms in molecules or solids, possessing electrons with unpaired spins. We can therefore study with the EPR technique:

1. atoms or ions with incomplete inner shells, e.g. transition metal atoms, rare earth atoms and actinides.

2. atoms, molecules and lattice defects with odd numbers of electrons, e.g. free sodium atoms, organic free radicals.

3. metals.

This selection is contrasted by the atoms suitable for NMR spectroscopy, where diamagnetic behavior is required. Although we are especially interested in the 3-d transition metal ions let us first illustrate the principles of resonance taking a free electron as a system. Consider an electron with magnetic moment $\vec{\mu}$ and spin $\hbar\vec{s} = \hbar/2$. The two quantities magnetic moment and spin momentum are antiparallel, and we may write

$$\vec{\mu} = -g\mu_B \vec{s} \tag{1}$$

with the Bohr magneton

$$\mu_B = \frac{e\hbar}{2m_e} = 9.27 \times 10^{-21} \quad \text{erg/gauss} \tag{2}$$

For a free electron s = 1/2 and g = 2.00232, therefore the spin magnetic moment of a free electron is closely equal to the Bohr magneton. In an applied magnetic field the energy levels of the system are given by

$$E = -\vec{\mu} \cdot \vec{H} \tag{3}$$

If $\vec{H} = H_o \hat{z}$, then

$$\begin{aligned} E &= -\mu_s H_o \\ &= g\mu_B m_s H_o \end{aligned} \tag{4}$$

The allowed values of m_s are $m_s = \pm 1/2$ with the energy eigen-values

$$E(m_s) = g\mu_B m_s H_o \tag{5}$$

In a magnetic field an electron with spin 1/2 has two energy levels corresponding to $m_s = \pm 1/2$:

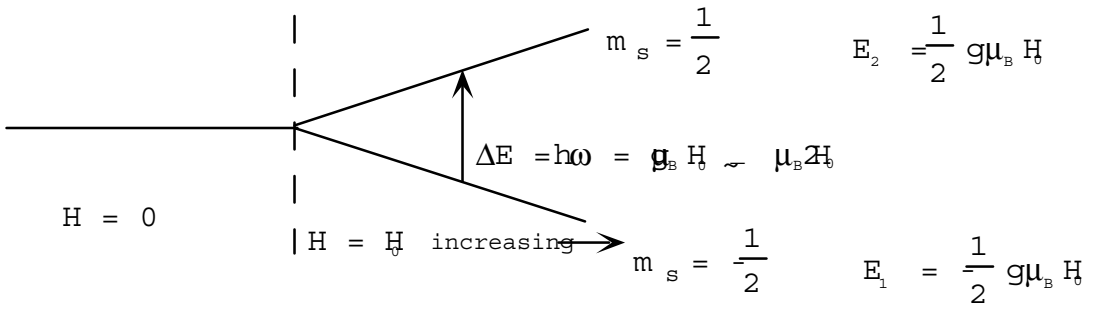

Fig. 1

The energy difference between the two levels is therefore:

$$\Delta E = h\upsilon = g\mu_B \ H_o \tag{5a}$$

This effect is called the electronic Zeeman effect. In terms of frequencies, the energy difference for the electron spin is:

$$\omega = \frac{\Delta E}{h} = \frac{g\mu_B H_o}{h} \tag{5b}$$

for the electron this reduces to:

$$\upsilon(\text{GHz}) = 2.80 \ H_o \ \text{(Kilo Gauss)}.$$

B. Detecting Resonance

Classically an external magnetic field H_o applied in the z direction exerts a torque on the electron dipoles, resulting in a precession of their moments about H_o.
The rate of precession is given by:

$$h\frac{d\vec{s}}{dt} = \vec{\mu} \times \vec{H} \tag{6}$$

and with Eq. (1):

$$\frac{d\vec{\mu}}{dt} = -\frac{g\mu_B}{h}(\vec{\mu} \times \vec{H})$$

Because $\vec{H} = (0, 0, H_o)$ we have:

$$\begin{aligned} \dot{\mu}_x &= -\frac{g\mu_B\mu_y H_o}{h} \\ \dot{\mu}_y &= +\frac{g\mu_B\mu_x H_o}{h} \\ \dot{\mu}_z &= 0 \end{aligned} \qquad (7)$$

An additional term could be added to these equations to include damping. In the absence of damping Eq. 7 have the solutions:

$$\begin{aligned} \mu_x &= \mu_o \cos \omega_o t \\ \mu_y &= \mu_o \sin \omega_0 t \\ \mu_z &= \text{constant} \end{aligned} \qquad (8)$$

with $\omega_o = g\frac{\mu_B}{h} H_o$ as in Eq. (5b).

If a circularly polarized oscillating magnetic field is applied perpendicular to z so that it rotates about H_o in the same sense, and with the same angular frequency as the precessing moment vector, it will cause the dipole to reverse its direction. This corresponds to an exchange of energy between the transverse oscillatory field and the magnetic system. It occurs only when the frequency of oscillation coincides with the precession frequency, ω_o (Eq. 5b), which is referred to as the resonant frequency. The oscillatory field is produced in a microwave cavity which serves to concentrate the r.f. field. The microwave source is tuned to the cavity resonant frequency and kept constant while the magnetic field is varied until the resonance condition Eq. 5 is satisfied. This may be detected by measuring a change in the cavity Q-factor when microwave power is absorbed by the magnetic system. This will be discussed in more detail in Part IV.

Revised 1/1993.

C. Spin-Lattice Relaxation

If both levels in Fig.1 are equally populated the probability for absorption and stimulated emission of absorption of radiation in resonance is exactly equal. This means that, per time interval, there is an equal amount of spin-up and spin-down flips and there will be no net absorption of energy. However in thermal equilibrium, the populations are determined by the Boltzmann distribution function, such that the population of the upper (2) and lower (1) level is determined by:

$$N_{1,2} = N_o \, e^{-\left(\frac{E_{1,2}}{k_B T}\right)} \tag{9}$$

and the ratio is

$$\frac{N_2}{N_1} = e^{-\left(\frac{E_2 - E_1}{k_B T}\right)}$$

$$= e^{\frac{h\omega_o}{k_B T}} < 1 \tag{10}$$

where T is the temperature of the system in Kelvin and k_B is the Boltzmann constant.

We may define polarization by

$$p = \frac{N_1 - N_2}{N_1 + N_2} = \frac{N_1 - N_2}{N} \tag{11}$$

With Eq. (9), the polarization under thermal equilibrium can be derived:

$$p_o = \tanh \frac{h\omega_o}{k_B T} \tag{12}$$

For $h\omega_o << k_B T$, which is usually a good approximation down to temperatures of about 4°K, we find:

$$p_o \approx \frac{1}{2} \frac{h\omega_o}{k_B T} \tag{13}$$

Revised 1/1993.

Thus under thermal equilibrium $N_1 > N_2$, resulting in an excess of upward transitions and a net absorption of energy P from the r.f. field, which is proportional to the differences of N_1 and N_2:

$$\begin{aligned} P &= (N_1 - N_2)\, h\omega_o r \\ &= N p h\omega_o r \end{aligned} \qquad (14)$$

where r is the spin-flip rate (# flips/sec).

Under continuous absorption of energy we will finally end up with $N_1 = N_2$ ($p = 0$) and the net absorption of energy will tend to zero. The magnetic system can then absorb no more power and is said to be saturated.

That this does not occur in general is due to the coupling between the magnetic system (or spin system) and the crystal lattice containing the spins. The upward spin-flip due to energy absorption brings the system out of thermal equilibrium. Spin-lattice relaxation provides a path back from the upper to the lower level and, as it is a non-radiative process, it is not governed by the radiation laws mentioned above. The return to the ground state proceeds usually by emission of a phonon of energy $h\omega_o$ (direct process):

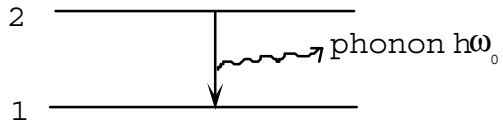

The down-flip happens with a rate $\frac{1}{T_1}$, where T_1 is called the spin-lattice relaxation time. The two effects of absorption and relaxation complete, and the net change in polarization is given by the rate equation:

$$\dot{P} = -\frac{(p - p_o)}{T_1} - pr \qquad (15)$$

which has the steady state solution:

$$p = p_o\,(1 + rT_1)^{-1} \qquad (16)$$

Revised 1/1993.

For $rT_1 << 1$ (low r.f. power or short relaxation times) $p \approx p_o$, but if $rT_1 >> 1$, p is reduced and therefore also the EPR signal. The term rT_1, is called saturation parameter.

Spin-Lattice relaxation is also important in that it may cause line broadening in a resonance experiment. The line width can be estimated with the uncertainty relation:

$$\Delta E \Delta t \sim h$$

where we identify Δt with T_1:

$$\Delta\omega_o = \frac{g\mu_B}{h} \Delta H_o \sim \frac{1}{T_1} \qquad (17)$$

Usually T_1 is rather small at room temperature and EPR signals can not be detected. Then the sample must be cooled, and for many paramagnetic ions it is necessary to go to 20°K or below in order to detect resonance at all.

Beside the spin-lattice relaxation, the spin-spin interaction leads also to line broadening. To reduce this contribution to the line width, the paramagnetic ions are usually diluted in a diamagnetic salt, which increases the distance between the spins.

IV. INSTRUMENTATION

The experimental set-up of the EPR spectrometer used in the 303 lab is outlined in Fig. 2.

The spectrometer consists of two main parts: the microwave bridge, and the receiving system with the magnets.

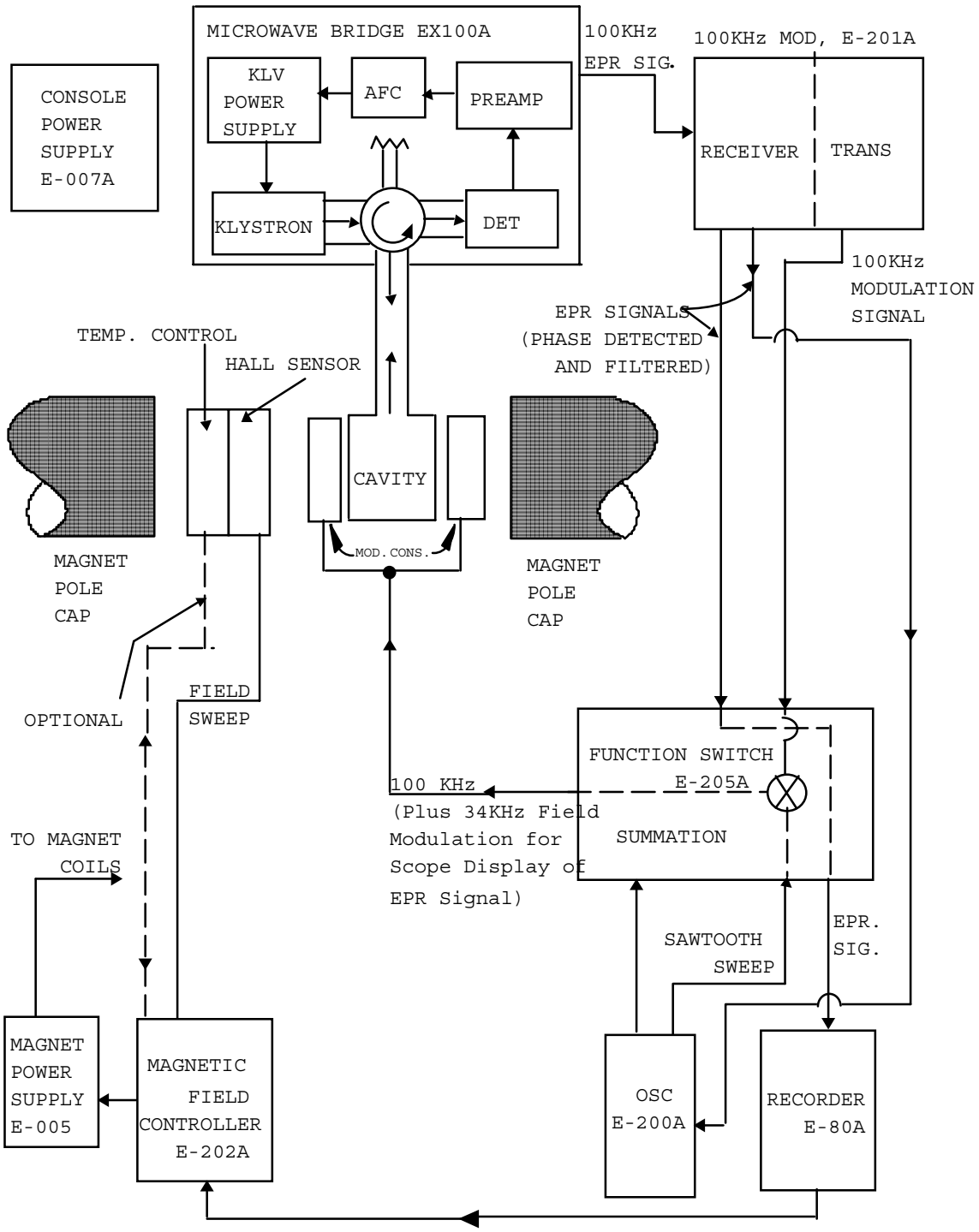

Fig. 2 E-4 System Block Diagram

A. The Microwave bridge

The microwave bridge serves the function of generating microwaves and detecting the EPR signal.

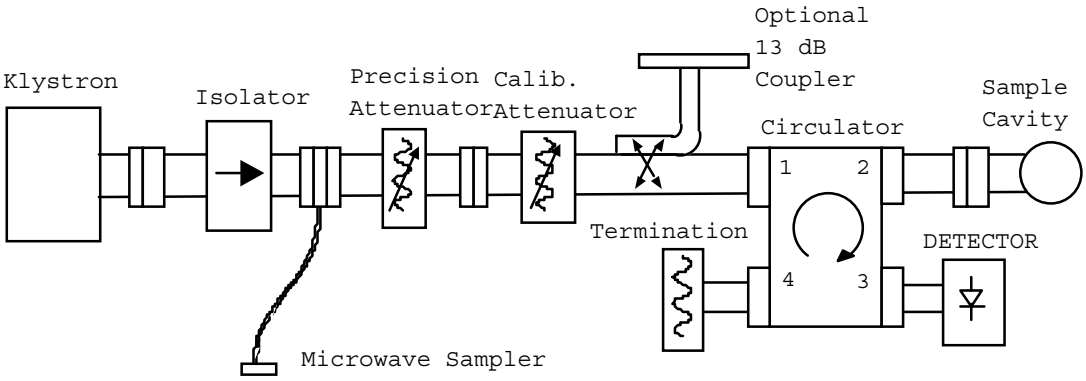

Fig. 3

Klystron: The klystron oscillator generates the microwave energy in the frequency range of 8.8 to 9.6 GHz (x-band frequency range) for sample excitation. The klystron frequency can be controlled by the front panel FREQUENCY knob.

Attenuator: The klystron output is fed to an attenuator to adjust the microwave power. The attenuator has a front panel ATTENUATOR/POWER control to indicate microwave energy incident upon the sample cavity.

Circulator: The circulator operates in two ways: it directs the attenuated microwave power to the sample cavity and reflected energy from the cavity back to the crystal detector.

Sample Cavity: The resonant sample cavity acts like a tuned circuit which has a very high Q (≈ 5000), where Q is defined as:

$$Q = \frac{\omega \times \text{Energy stored}}{\text{Power dissipated in cavity}}$$

Revised 1/1993.

When a resonance is obtained from the sample, the impedance of the cavity is changed and a signal is reflected to the crystal detector.

In our experiment a rectangular cavity is employed with TE_{102} operation mode, resonating at 9.5 GHz. The electromagnetic field configuration in the resonance cavity is shown in Fig. 4a, and a cross section through the cavity containing a sample tube is shown in Fig. 4b. The sample is sitting at the position of highest magnetic field H_l, and is polarized normal to the main field direction H_o. The field H_l is oscillating linearly. However, a linearly oscillating field is equivalent to two fields rotating in opposite directions. The component rotating in the same direction as the precessing spins will be in resonance and may cause transitions; the other component is out of phase and does not affect the spin system.

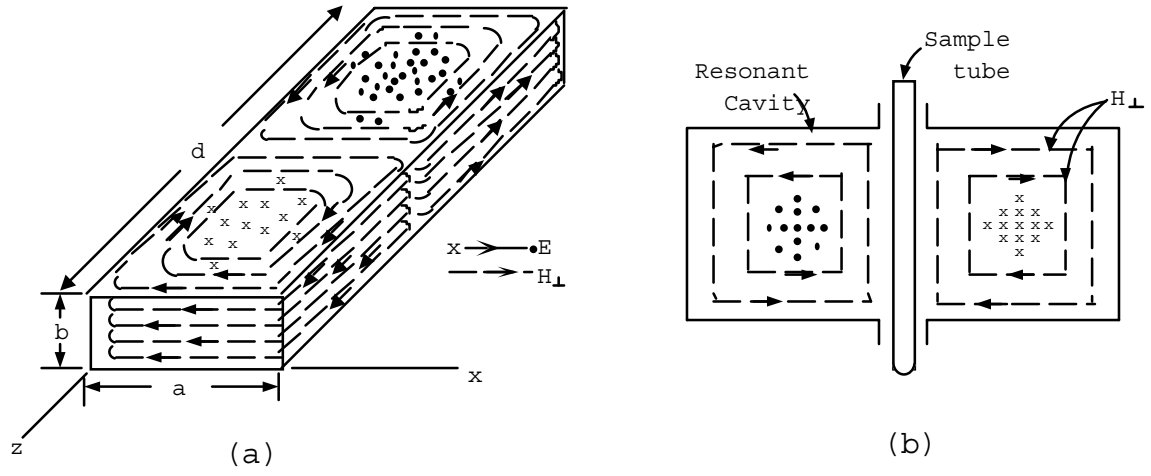

Fig. 4

For each sample the cavity resonance frequency must be tuned separately. This is done in the TUNE mode of the klystron, after the ATTENUATION/POWER is set to about 25dB. Once tuned, an automatic frequency control (A.F.C.) locks the klystron frequency to the sample cavity resonant frequency in the OPERATION mode.

Detector: will be discussed in the next section.

B. The magnetic field scan

As already mentioned, in an EPR experiment the microwave frequency is kept constant and the external magnetic field is swept through the resonance condition. The sweep is provided by a saw tooth generator and the magnetic field is simultaneously monitored by a Hall probe. This is easier done than to sweep the microwave frequency since most microwave components have a fairly narrow band performance.

The sweep of the magnetic field will give one resonance if the fixed cavity frequency corresponds to the energy splitting:

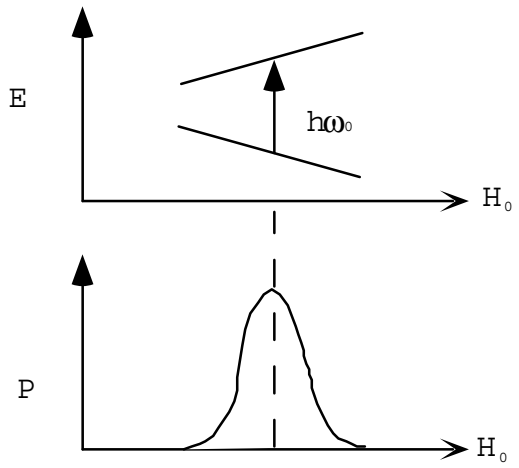

Fig. 5

The center of the magnetic field sweep can be set by the console control FIELD SET and the width of the magnetic field to be scanned is set by SCAN RANGE. The scan is symmetrical about the center field value indicated by the FIELD SET control. The magnetic field is recorded by the x-axis of the chart-recorder.

For reasons of better amplification and recording the EPR signal one usually superimposes a high frequency modulated magnetic field on top of the slow swept magnetic field. The h.f. modulation is applied by means of small coils mounted outside the cavity walls, and has usually a frequency of 100 KHz. The modulation amplitude is kept smaller than the resonance line width. Under these circumstances the detected signal

is proportional to the slope of the absorption curve, while the steady field is swept slowly through the resonance as shown in Fig. 6.:

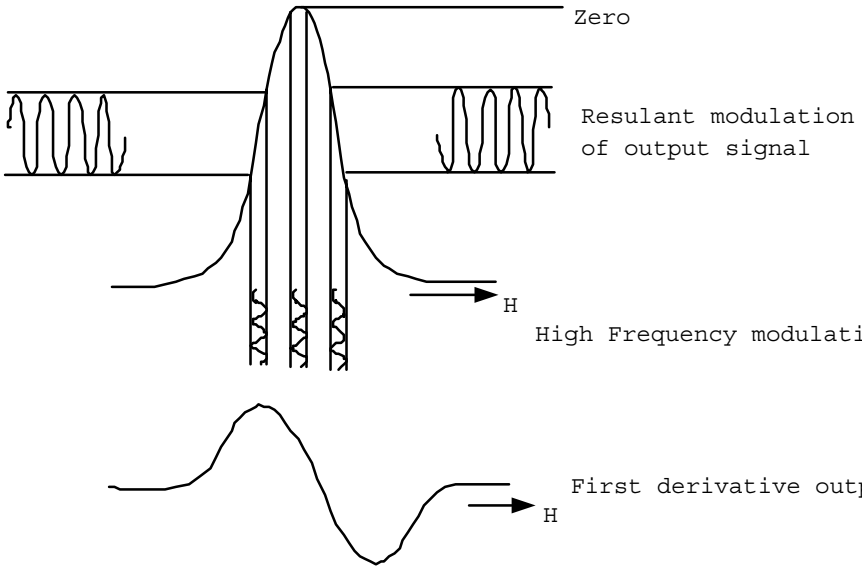

Fig. 6. Generation of EPR signal.

The phase and amplitude of this modulation is dependent on the EPR resonance line and the value H_o relative to the resonance line. The modulated microwave energy strikes the crystal diode in one arm of the circulator. If the signal were then detected by a simple rectifier the output would then have the form of the positive half of Fig. 7a. But, in practice, it is usual to employ phase-sensitive detection which takes care of the sign of the slope and gives a true differential of the line shape as shown in Fig. 7b.

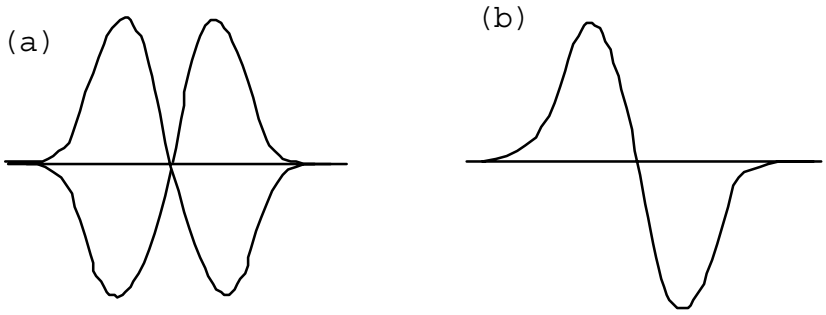

Fig. 7 EPR signal (a) at the diode, (b) after phase detection.

Revised 1/1993.

The signal is now ready for amplification (RECEIVED GAIN) and demodulation, and the signal output is fed to the y-axis of the pen-recorder. With the front panel knob MODULATION AMPLITUDE the 100 KHz modulation amplitude is controlled. If the amplitude is infinitely small, a true first derivative curve will result. But then the signal level will be very small. Therefore the modulation amplitude must be increased somewhat, and as a rough rule of thumb a modulation amplitude equal to 1/10 of the signal line width is usually adequate.

V. EPR SPECTRUM OF V^{2+}

One of the most widely used applications of EPR is the study of paramagnetic ions in solids, especially ions in solids, and in crystals of various kinds. Ions with an unpaired electron spin such as the iron group vanadium, manganese, cobalt, iron, chromium, copper and nickel, each give a characteristic spectrum depending upon their valence state as well as a characteristic hyperfine structures (dependent upon nuclear spin). These ions as impurities in a crystal can be identified, and very often information about the environment around the ion can be obtained. Because of crystal field splitting the symmetry of the site occupied by the ion is most important. Quite obviously these are complex effects, therefore we have picked a fairly simple yet representative case, V^{2+} whose paramagnetism arises from the unfilled $3d^3$ atomic shell. You will observe the spectrum for a dilute solution of V^{2+} ions substituting for Mg^{2+} ions in MgO. Magnesium oxide has the NaCl structure, therefore a highly symmetric octahedral symmetry at the cation site.

A closely related ion is Cr^{3+} which also has the $3d^3$ configuration. Chromium in sapphire gives rise to the well known red color of ruby. The crystal field splitting in this case is more complicated because of the lower axial symmetry of sapphire.

Returning to the case of V^{2+} in MgO, we first have to consider the ground state of the $3d^3$ ion then the splitting of these ground state energy levels by the octahedral crystal field. All three electrons in the unfilled d shell have orbital quantum numbers $l = 2$ and spin quantum numbers m_s ($\pm 1/2$). For each electron there are $2l + 1$ orbital states, each characterized by magnetic quantum number m_l and for each of these there are $(2s + 1)$ spin states characterized by m_s. In calculating electronic energies the Coulomb and exchange interactions between electrons slightly modify the atomic shell energies depending upon the final terms ^3F, ^3P, ^1G, ^1D, ^1S etc., depending upon the way the

electrons combine in the shell. In Russel-Saunders or L-S coupling the electrons are coupled together to form a system with total orbital quantum number L and total spin quantum number S. The total angular momentum quantum number J including spin-orbit coupling is then obtained by vectorial addition of L and S. The states with lowest energy are those with minimum J in the lower half of an unfilled shell and maximum J in the upper half. Of the various terms possible the one with lowest energy is given by Hund's rules, and this is the term we are interested in. According to Hund's rules the lowest energy term is that having (1) maximum total spin and (2) maximum total orbital momentum consistent with (1). Thus the lowest term value for V^{2+} is found by placing the three electrons of the l=2 shell as indicated in Table I.

Table I. m_s and m_l for the three electrons in the lowest energy state ^4F of V^{2+}

Electron	1	2	3	
m_s	1/2	1/2	1/2	S = 3/2 (M_S = 3/2, 1/2, -1/2, -3/2)
m_l	2	1	0	L = 3 (M_l = 3, 2, 1, 0, -1, -2, -3)

There is, therefore, a four-fold spin and a seven-fold orbital degeneracy.

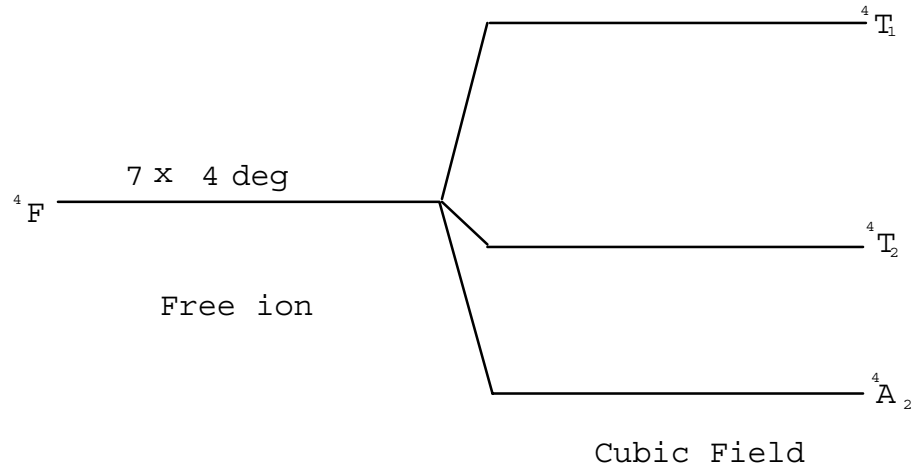

Fig. 8

Now when this ion is placed in an octahedral crystal field (as in the MgO crystal), the orbital degeneracy is split into a singlet and two triplets (see reference 2). Refer to Fig. 8.

Actually, the singlet state $^4A_2$ is lowest by a considerable amount $\sim 10^4$ cm^{-1}. At ordinary temperatures only the singlet level is occupied and magnetism arises from spin only. The four fold M_S spin degeneracy is unaffected by the cubic crystal field. Thus in this special case we deal with spin only magnetism.

There are small second order spin-orbit effects which influence the magnetic properties of the ion. These can be taken into account by an effective g factor, usually in the range of values g = 1.97 to 1.99. Here the g-factor is isotropic or nearly so.

A so called spin Hamiltonian is defined by

$$H = g\mu_B \vec{H} \cdot \vec{S} \qquad (18)$$

where the vector $\vec{S}$ is spatially quantized. For spin S = 3/2, 2S + 1 = 4 levels result described by m_S = 1/2, -1/2, 1/2 and 3/2. More precisely, it is convenient to take the magnetic field H in the z direction. The spin Hamiltonian reduces to $H = g\mu_B HS_Z$ where the operator S_Z is one of the Pauli spin matrices for S = 3/2. Sz is diagonal and the eigenvalues in the problem can be readily obtained (refer to ref. 2) leading to four energies linearly dependent upon H as follows:

$$E_{\pm\frac{1}{2}} = \pm\frac{1}{2} g\mu_B H$$
$$E_{\pm\frac{3}{2}} = \pm\frac{3}{2} g\mu_B H \qquad (19)$$

In a magnetic resonance experiment, transitions take place between the four levels according to $\Delta m_S = \pm 1$ as shown in Fig. 9. Here in the absence of hyperfine and crystal field splitting, the various allowed transitions (M_S = -3/2 → - 1/2, -1/2 → 1/2 and 1/2 → 3/2) are coincident in energy and one resonance line results.

Revised 1/1993.

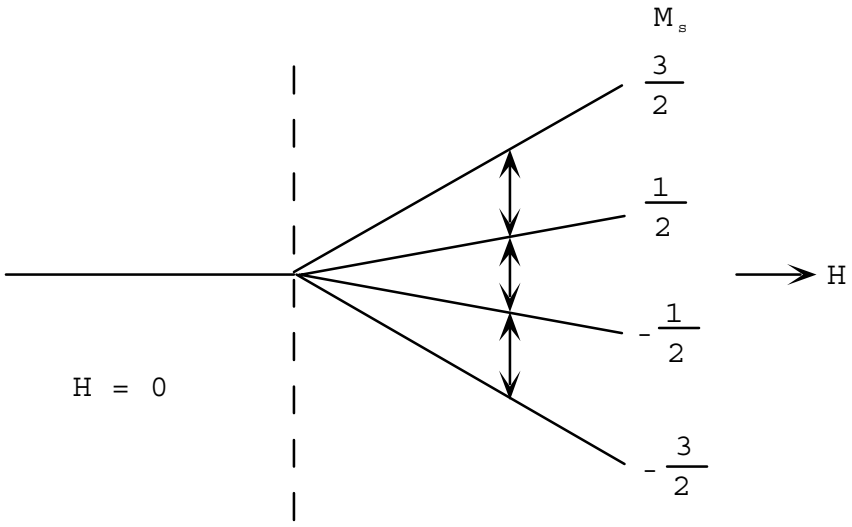

Fig. 9

Actually Cr^{3+} in MgO has a very small hyperfine splitting and nearly fits this case. Our samples contain a small amount of Cr which gives rise to a weak central line or spectrum.

Vanadium, however, has a strong hyperfine splitting due to interaction between the electronic moment s = 3/2 and the magnetic moment of its nucleus (nucleus spin quantum number I = 7/2). One way to look at this is to think of the nuclear moment as producing a magnetic field in the vicinity of the atomic electrons. Because of the relatively small distance between electrons and nucleus ($\sim$ 0.5A), a strong dipole-dipole interaction results leading to splitting of the ground state levels involved. The Hamiltonian Eq. 18 must be modified to include these effects of nuclear spin $\vec{I}$, gyromagnetic ratio g_N and nuclear magneton $\mu_N = 5.05 \times 10^{-24}$ erg/gauss:

$$H = g\mu_B \vec{H} \cdot \vec{S} + A\vec{I} \cdot \vec{S} + g_N \mu_N \vec{H} \cdot \vec{I} \qquad (20)$$

Here the second term leads to the hyperfine splitting and the last term represents the magnetic energy of the nucleus in the magnetic field. It turns out that the last term can be neglected relative to the other two terms (mainly because μ_N is so much smaller than μ_B).

Revised 1/1993.

As before the spin operators can be utilized to set up the eigen problem for the alignment of the nuclear moment in the field of the electrons. Again $\vec{I}$ is spacially quantized and can take up (2I + 1) positions relative to $\vec{S}$. For V^{2+}, I = 7/2 and this leads to 8 equally spaced levels for each M_S value. The eigenvalues are of the form

$$E(M_S, M_I) = g\mu_B H_Z M_S + A M_S M_I \qquad (21)$$

These levels are designated by M_S and a quantum number M_I = 7/2, 5/2, 3/2, 1/2, -1/2, -3/2, -5/2 and -7/2. Figure 10 shows just two of the Ms = ± 1/2 energy levels of the system plotted against increasing magnetic field. At resonance the microwave field induced transitions as shown by the arrows according to $\Delta M_I = 0$ and $\Delta M_S = \pm 1$. Eight hyperfine lines result as indicated. You should readily observe these and determine the separation in gauss $H_{M_I-1} - H_{M_I}$ between adjacent components.

From Eq. 21 and Fig. 10 you should be able to show that the separation between adjacent hyperfine levels in gauss is given by

$$\Delta H = H_{M_I-1} - H_{M_I} = \frac{1}{g\mu_B} A \qquad (22)$$

where A is the hyperfine splitting constant used in Eq. 21. ΔH can be precisely measured and, providing the effective g factor is well known, A can be determined quite accurately. For V^{2+} you should find a value somewhere in the range 50 to 100 $\times 10^{-4}$ ($1\ cm^{-1} = 1.99 \times 10^{-16}$ erg).

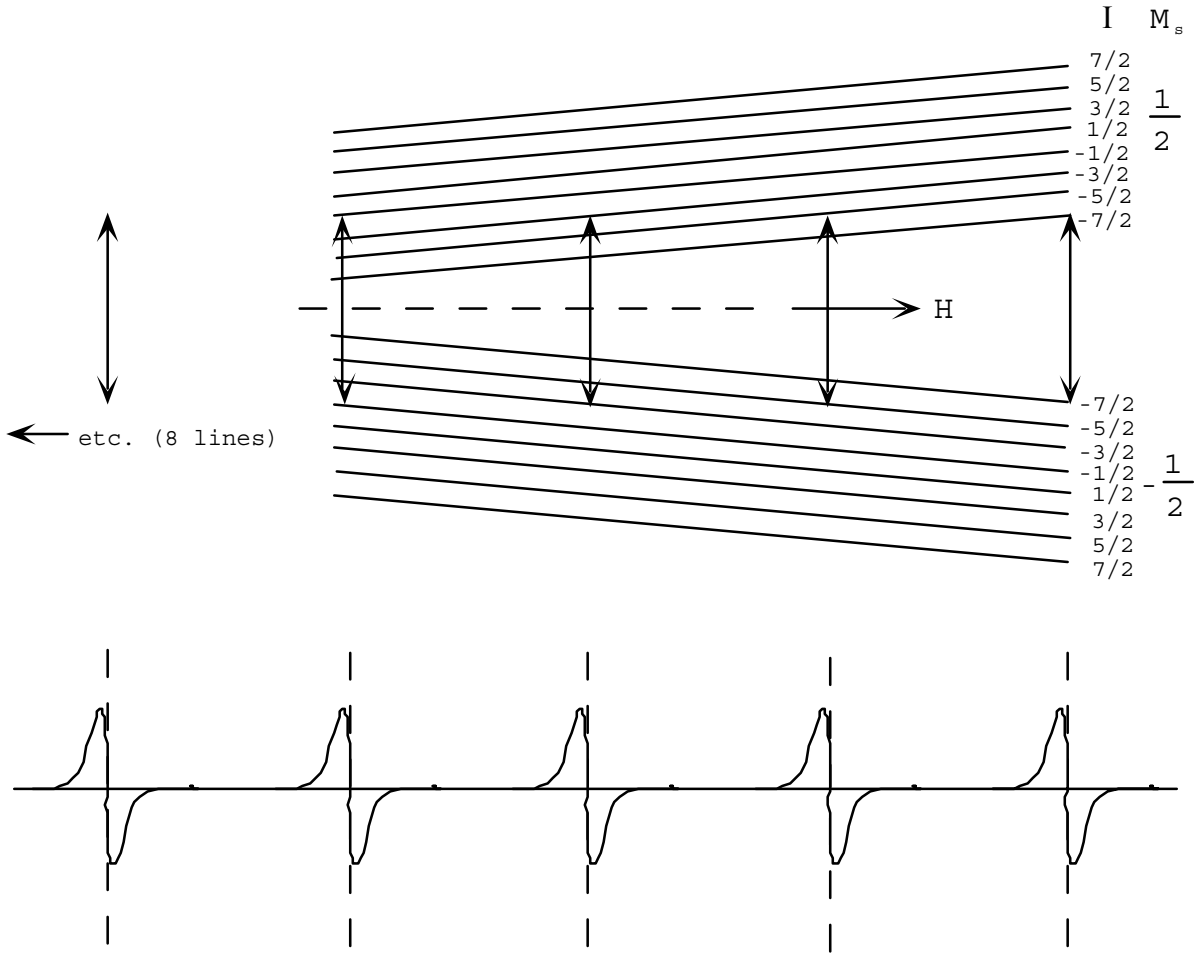

Fig. 10

VI. PROCEDURE

A. Operation and Startup

Preparation:

1. Position a sheet of calibrated chart paper on the recorder platen with the center line of the chart aligned with the red arrow on the top of the platen. The paper is held in place by a vacuum mechanism in the base under the paper. The recorder must be switched ON for the vacuum mechanism to function.

2. Fill and assemble the pen. Simply place one of the small colored markers in the metal ring attached to the recorder arm.

PRE-OPERATION SETTINGS

1. Set bridge MODE to STANDBY

2. Set RECORDER/ON-OFF to OFF.

SYSTEM TURN-ON

1. Open coolant water supply valve(s) to E-4 coolant system. You also must flip a switch on the magnet cooling apparatus on the floor just to the left of the EPR unit. There is an overall system power switch located on the lower left end of the face of the recorder unit (the unit that has the recording arm and chart paper), just below the SCAN RANGE control knob. This overall power switch must be ON.

Preliminary Adjustments:

INSERTING THE SAMPLE

Wipe sample tube with a lint-free cloth. Insert the organic free radical sample (DPPH) in the cavity to the rubber ring so the active volume is centered in the cavity. Refer to REFERENCE INFORMATION section for EPR cavity details.

BRIDGE TUNING

PLEASE NOTE: Control settings differ for various samples. Settings in this procedure are for DPPH sample 904450-01 which produces a large signal to simplify location.

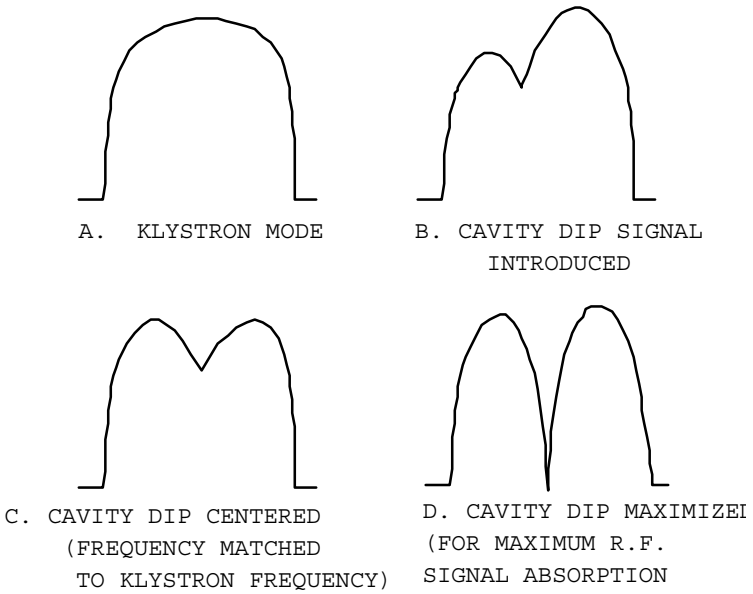

Fig.11 Oscilloscope tune mode traces

1. Set ATTENUATION/POWER at 25dB and turn MODE switch to TUNE (klystron mode trace will then appear on oscilloscope).

2. Adjust FREQUENCY control until cavity signal dip is centered at highest point of klystron mode trace.

3. Adjust cavity coupling iris (white teflon screw) to the point where maximum dip is obtained.

4. Turn MODE switch to OPERATE.

PLEASE NOTE: The AFC is now on, and the klystron should be locked to the cavity frequency. Verification of the AFC lock can be made by rotating the FREQUENCY control back and forth through a small excursion of the dial and checking the AFC output follows these excursions.

Revised 1/1993.

5. Slowly rotate ATTENUATOR/POWER control to approximately 10 dB and simultaneously keep DETECTOR CURRENT at 300 μA by adjusting iris screw on cavity as necessary.

6. Adjust FREQUENCY control on bridge to a setting that yields maximum detector current. At this point the AFC output should be nearly zero. If the AFC output meter exceeds ± 10 V, refer to MAINTENANCE, paragraph 6.4.6, Reflector Tracking Adjustment.

MODULATION SETTINGS

1. Set MODULATION AMPLITUDE to 6.3 Gauss (0.63 x 10 raised to the first power) and RECEIVER GAIN to 5.0 x 10 raised to the second power.

FIELD CONTROL SETTINGS

1. Set SCAN RANGE to OFF and FIELD SET/THOUSANDS switch to 3 kiloGauss. Adjust FIELD SET/UNITS to 400 Gauss. Find the resonance by watching the DETECTOR LEVEL and adjusting FIELD SET/UNITS.

Recording a spectrum:

1. On recorder set SCAN MODE to SINGLE.

2. Press recorder left FAST SCAN or NORMAL SCAN button (pen carriage moves to left side of recorder).

3. On recorder, set PEN MODE to AUTO and SCAN TIME to 0.5 min.

4. Set field control SCAN RANGE to 40 GAUSS.

5. Set RECORDER/ON-OFF to ON.

6. Adjust modulation module RECORDER PEN POS to center recorder pen on chart.

7. Set modulation module SIGNAL FILTER to 1.0 SEC.

8. Momentarily press the RIGHT SCAN switch (EPR signal records on the chart).

Changing the sample:

CAUTION: Before removing sample from cavity always reduce microwave power using ATTENUATION/POWER control on bridge or excessive current may damage detector crystal.

1. Turn bridge ATTENUATION/POWER to reduce microwave power to 25dB (approx.).

2. Turn bridge MODE to TUNE.

3. Remove sample from cavity.

System Shutdown:

CAUTION: To avoid damaging the detector crystal always turn off system power in the order given.

1. Set RECORDER/ON-OFF to OFF.

2. Turn bridge ATTENUATION/POWER control to minimum power (25dB).

3. Set bridge MODE to STANDBY.

4. Press console power switch.

5. If desired turn coolant water OFF.

B. Calibration with DPPH

Measure first the EPR spectrum of DPPH, The organic free radical DPPH, (CH) N - NC H (NO) shows a very strong and narrow isotropic resonance line due to a "free electron" associated with one of the nitrogen atoms. The g-value has been determined with high accuracy to be 2.0036 ± 0.0003 (for a really free electron g is 2.0023). Rather than to measure the frequency of the microwave and magnetic field to great accuracy, we use DPPH as a standard and determine the g-value of the unknown sample in relation to the g-factor of DPPH.

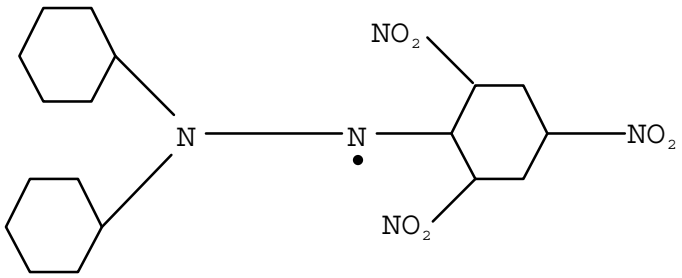

Fig. 12. Chemical structure of DPPH (diphenyl-picryl-hydrazil).

For this purpose it is useful to find the DPPH resonance g = 2.0036 and then take a number of repeated scans with decreasing modulation amplitude. If the spectrometer has a good uniform magnetic field, for a small sample the line width should approach an intrinsic value for DPPH at the smallest modulation amplitude. Attempt to find these conditions and when you do estimate the relaxation time T from the recorded line width. Be sure and note the magnetic field for the g = 2.0036 resonance and klystron frequency you are set to (keep this microwave frequency constant if you can).

C. Measurement of hyperfine structure of V^{2+} in MgO

Insert MgO crystalline sample number 1 which contains V^{2+} as a substitutional impurity. Remember this is a paramagnetic $3d^3$ ion with a ^4F ground state split by the cubic crystal field so that the lowest occupied state has S = 3/2. The spin of the V nucleus

is I = 7/2. We expect, and you should find, 8 hyperfine lines in the spectrum. From the g-factor (referred to DPPH) and the observed hyperfine splitting in gauss, find the hyperfine splitting constant in cm^{-1}. List your values and their accuracy in a table.

If you are well adjusted, a certain amount of fine structure will be evident on each hyperfine line. This is caused by a second order hyperfine term which is different for different M_s transitions. Refer to ref. 3. It is not dependent upon crystal orientation in $\vec{H}$ (rotate the sample take different scans) but the intensity of this fine structure may vary with angle.

You should also pick up other impurities at lower level in MgO sample #1. For example, the S = 3/2, I = 3/2 line of Cr^{3+} appear mainly as a central line with very small hyperfine splitting. The g value should be about g = 1.9800.

D. Suggestions for Further Work

There are many other samples to investigate with this versatile apparatus. Careful study of some of these would make a good individual project. A special case is that of EPR for Cr^{3+} in sapphire-single crystal ruby. This is an example where crystal field splitting is very important and most dependent upon orientation of the ruby crystal in the magnetic field. Samples of ruby which give good EPR signals are available but they should be carefully oriented using x-ray diffraction in order to make sense out of the many-line EPR spectra observable. See L. A. Collins, M. A. Morrison and P. L. Donoho, Amer. J. Physics 42, 560 (1974) for an advanced undergraduate EPR experiment on single crystal ruby (as well as further references).

A number of other materials are available which show good EPR signals. These include Cu_2SO_4:H_2O), MgO crystals containing Mn^{2+}, SmO, $GaNO_2$ and others. Also it is possible to produce color centers in crystals like the alkali halides KCl, KBr etc. and alkaline earth oxides (CaO) by exposure to penetrating x-rays. These so-called F-centers are paramagnetic. For further details see reference 4.

Revised 1/1993.